for plane hydrodynamics in the work of S. Kida [1], for 3D vortices – in the works of V. V. Zhmur and co-authors [2, 3], where the dynamics of vortices under various background conditions [2] was considered. It is shown that, under deformation, the vortex boundary has three variants of behavior: rotation, nutation oscillations, and unlimited elongation. The vortex behavior in a barotropic background flow and flows with vertical shear is different. Under certain conditions in the presence of a background flow, the vortex, deforming, can be stretched into a thread. In these theories, when a vortex is deformed, its boundary remains elliptical in the 2D case and ellipsoidal in the 3D case. When a vortex is stretched in a horizontal plane, i.e., with an increase in the longitudinal dimension relative to the transverse one, the fluid motion induced by it decreases. From a physical viewpoint, the regime of unlimited stretching corresponds to the vortex destruction by the flow.

The present work is aimed at studying the vortex energy during its transformation by stretching, as well as at verifying the theory by comparing the results with the estimates obtained from *in-situ* data.

A decrease in orbital velocities entails a decrease in the kinetic energy of the vortex. However, it turned out that when the vortex is elongated, the potential energy also decreases.

The total energy of the vortex in the ocean H is determined by the formula

$$H = \frac{1}{2}\iiint\left[\rho_{\Sigma}(x,y,z)\left(u^2(x,y,z)+v^2(x,y,z)\right)+\frac{g^2}{\rho_0(z)}\frac{\rho^2(x,y,z)}{N^2(x,y,z)}\right]dx\,dy\,dz\,, \quad (1)$$

where ρ_0 is mean sea water density by sea depth; u and v are zonal and meridional flow velocity components; g is free fall acceleration; N is the Väisälä-Brunt frequency; $\rho = (\rho_{\Sigma} - \rho_0)$ is the deviation of the current density ρ_{Σ} from ρ_0. The integration boundaries are determined by the vortex scales [4], and the horizontal boundaries are determined by the isolines of zero relative vorticity $\zeta = \frac{\partial v}{\partial x} - \frac{\partial u}{\partial y}$; over depth, the integral is taken from 0 to 1000 m. The first term in formula (1) is kinetic energy, the second is the available potential energy of the vortex.

Transformation formulas

The dimensionless parameter ε characterizes the vortex elongation degree and is determined through the ratio of its horizontal scales $\varepsilon = \frac{a}{b} \geq 1$, where a and b are horizontal semi-axes of the ellipsoid core: a is the major semi-axis, b is the minor

[2] Zhmur, V.V. and Pankratov, K.K., 1989. The Dynamics of the Semi-Ellipsoid Subsurface Vortex in the Non-uniform Flow. *Oceanology*, 29(2), pp. 205-211 (in Russian); Zhmur, V.V. and Pankratov, K.K., 1990. Dynamics of Submesoscale Eddy in a Flow Field of Large Strong Vortex. *Oceanology*, 30(2), pp. 170-178 (in Russian); Zhmur, V.V. and Pankratov, K.K., 1990. Distant Interaction of an Ensemble of Quasigeostrophic Ellipsoidal Eddies. Hamiltonian Formulation. *Izvestiya of the Academy of Sciences of the USSR. Atmospheric and Oceanic Physics*, 26(9), pp. 972-981 (in Russian).

semi-axis; c is the vertical semi-axis of the vortex. Using c, the dimensionless parameter of the vertical oblateness of the vortex core is introduced: $K = \frac{N}{f}\frac{c}{r_0}$, where $r_0 = \sqrt{ab}$ is the effective radius of the vortex; f is the Coriolis parameter; N is the Väisälä-Brunt frequency averaged over the depth in the 0–1000 m layer. It has been established that, when a vortex is deformed by a barotropic flow, the vertical semi-axis, as well as the product of the semi-axes a and b, and, accordingly, r_0 do not change. Consequently, the vertical oblateness parameter K of the core is also preserved when the vortex is deformed by a barotropic flow [2]. However, the latter is true under the assumption that the Väisälä-Brunt frequency is unchanged. If this frequency changes during the vortex life cycle, then the vertical oblateness parameter of the vortex core K will change accordingly.

Using nontrivial transformations, the formula for energy (1) can be transformed as dependence on ε and the oblateness parameter K, and there are several equivalent versions of formulas for the dependence of the total vortex energy as a (ε, K) function [2, 5–12]. Below, two variants for energy ratios identical to each other are shown:

$$H(\varepsilon, K) = \frac{2}{15}\pi\rho_0 r_0^3 c^2 \sigma^2 \frac{N}{f}\int_0^\infty \frac{d\mu}{\sqrt{\left(\mu^2 + \nu\mu + 1\right)\left(K^2 + \mu\right)}}, \tag{2}$$

$$H(\varepsilon, K) = \frac{3}{40\pi}\rho_0 \frac{V_0^2 \sigma^2}{c} K\int_0^\infty \frac{d\mu}{\sqrt{\left(\mu^2 + \nu\mu + 1\right)\left(K^2 + \mu\right)}}. \tag{3}$$

Here σ is potential vorticity according to Rossby [3]; $\nu = \varepsilon + \frac{1}{\varepsilon} \geq 2$ – another dimensionless parameter of horizontal vortex elongation; $V_0 = \frac{4}{3}\pi abc$ is the vortex core volume. In a coordinate system with two horizontal axes (x, y) and a vertical z-axis, the potential vorticity σ is expressed in terms of the stream function $\psi(x, y, z, t)$, where t is time [13]:

$$\sigma = \Delta_h \psi(x, y, z, t) + \frac{\partial}{\partial z}\frac{f^2}{N^2}\frac{\partial \psi(x, y, z, t)}{\partial z}.$$

Here $\Delta_h \psi = \mathrm{rot}_z \vec{u}$. The Väisälä-Brunt frequency $N(z)$ generally depends on the vertical coordinate z. The longer the vortex, the greater ε, and ν. Thus, long vortices correspond to very large values of ε and ν and, consequently, to lower energy.

Formulas (2) and (3) take into account the total energy of the vortex, including the kinetic and available potential energy of the core, as well as the energy of the external fluid trapped in the vortex motion. The theory of ellipsoidal vortices [2] makes it possible to calculate separately the kinetic, available potential, and total energy of the vortex core. The total mechanical energy H_{core}, as well as the kinetic

H^k_{core} and available potential energy of the vortex H^p_{core} contained in the vortex core volume, can be represented as functions of the parameters (ε, *K*). As a result of analytical calculations, the following relations at the output are obtained:

– the kinetic energy of the vortex core

$$H^k_{core}(\varepsilon,K)=\frac{1}{40}\rho_0\sigma^2V_0\ a\ b\ K^2\left\{\varepsilon\left(\int_0^\infty\frac{1}{\varepsilon+\mu}\frac{d\mu}{\sqrt{(\varepsilon+\mu)\left(\frac{1}{\varepsilon}+\mu\right)\left(K^2+\mu\right)}}\right)^2+\right.$$
$$\left.+\frac{1}{\varepsilon}\left(\int_0^\infty\frac{1}{\frac{1}{\varepsilon}+\mu}\frac{d\mu}{\sqrt{(\varepsilon+\mu)\left(\frac{1}{\varepsilon}+\mu\right)\left(K^2+\mu\right)}}\right)^2\right\}, \quad (4)$$

– the available potential energy of the vortex core

$$H^p_{core}(\varepsilon,K)=\frac{1}{40}\rho_0\sigma^2V_0\ a\ b\ K^4\left(\int_0^\infty\frac{1}{K^2+\mu}\frac{d\mu}{\sqrt{(\varepsilon+\mu)\left(\frac{1}{\varepsilon}+\mu\right)\left(K^2+\mu\right)}}\right)^2, \quad (5)$$

– the mechanical energy of the vortex core

$$H_{core}=H^k_{core}+H^p_{core},$$

where

$$H_{core}(\varepsilon,K)=\frac{1}{40}\rho_0\sigma^2V_0\ a\ b\ K^2\left\{\varepsilon\left(\int_0^\infty\frac{1}{\varepsilon+\mu}\frac{d\mu}{\sqrt{(\varepsilon+\mu)\left(\frac{1}{\varepsilon}+\mu\right)\left(K^2+\mu\right)}}\right)^2+\right.$$
$$+\frac{1}{\varepsilon}\left(\int_0^\infty\frac{1}{\frac{1}{\varepsilon}+\mu}\frac{d\mu}{\sqrt{(\varepsilon+\mu)\left(\frac{1}{\varepsilon}+\mu\right)\left(K^2+\mu\right)}}\right)^2+$$
$$\left.+K^2\left(\int_0^\infty\frac{1}{K^2+\mu}\frac{d\mu}{\sqrt{(\varepsilon+\mu)\left(\frac{1}{\varepsilon}+\mu\right)\left(K^2+\mu\right)}}\right)^2\right\}. \quad (6)$$

According to the theory, when a vortex is elongated by a barotropic flow, only *v* or ε changes in integrals (2) – (6), while all other characteristics do not change.

As the vortex elongates, the denominator in the integrand increases, which means that the integral itself decreases with elongation. This means that when the vortex is elongated, both the kinetic and available potential energy, as well as the mechanical energy of the vortex core, decrease. The maximum energy value (2) – (6) at a fixed K value corresponds to round vortices with $\varepsilon = 1$ or $\nu = 2$. When the Väisälä-Brunt background frequency changes, the K parameter will also change.

The mesoscale vortex evolution located in the Lofoten basin of the Norwegian Sea is considered for the study. Being a topographically isolated area, the Lofoten basin creates favorable conditions for the generation of many mesoscale vortices [14, 15]. The vortices extract part of the warm and salty Atlantic water from the Norwegian current branches and redistribute it throughout the basin [3]. Due to the vortex activity, the Lofoten basin is one of the most dynamically active regions of the World Ocean [4]. Its energy was considered in [16].

Among the many mesoscale vortices of the Lofoten basin, a vortex significantly changing its shape during its life cycle was chosen for analysis. The vortex under study existed on April 4–24, 2012, and during three weeks of evolution changed its shape from horizontally round to elongated, so that its longitudinal scale became several times larger than the transverse one. The present paper analyzes the graphs of the kinetic and potential energy of the vortex and other characteristics.

Data and method of identification

For the study, the data from the GLORYS12V1 global oceanic reanalysis is used. The array is provided by the Copernicus Marine Service (CMEMS). The data has a spatial resolution of 1/12° in latitude and longitude and 50 vertical levels, which allows them to be successfully used to study the World Ocean mesoscale structures. The GLORYS12V1 reanalysis assimilates along-track data from high-resolution altimeters as well as satellite observations of sea surface temperature, sea ice concentration, and *in-situ* temperature and salinity profiles. The basis of the reanalysis is the NEMO model, where the ECMWF ERA-Interim reanalysis is used as a forcing. The temporal resolution of the data is 24 hours.

Since the GLORYS12V1 data widely use the assimilation of satellite and *in-situ* information, they are referred to as "*in-situ* data" in this work.

Results

Fig. 1 shows the life cycle of a mesoscale anticyclonic vortex in the Lofoten basin in terms of relative vorticity. To visualize the region of the analyzed vortex and exclude fragments of other hydrodynamic structures, masks were constructed for each moment of time. The sequence of images allows tracing the vortex evolution, in which its shape is stretched. It can be seen that at the beginning of

[3] Belonenko, T., Zinchenko, V., Gordeeva, S. and Raj, R.P., 2020. Evaluation of Heat and Salt Transports by Mesoscale Eddies in the Lofoten Basin. *Russian Journal of Earth Sciences*, 20(6), ES6011. doi:10.2205/2020ES000720

[4] Volkov, D.L., Belonenko, T.V. and Foux, V.R., 2013. Puzzling over the Dynamics of the Lofoten Basin – A Sub-Arctic Hot Spot of Ocean Variability. *Geophysical Research Letters*, 40(4), pp. 738-743. doi:10.1002/grl.50126

the cycle, on April 4, 2012, the vortex is horizontally round, but gradually it begins to elongate so that by April 18 its length is several times greater than its width. By April 21, 2012, the vortex is even more stretched in the longitudinal direction, and by April 24, bending under the influence of currents, the vortex has the shape of a horseshoe on the horizon.

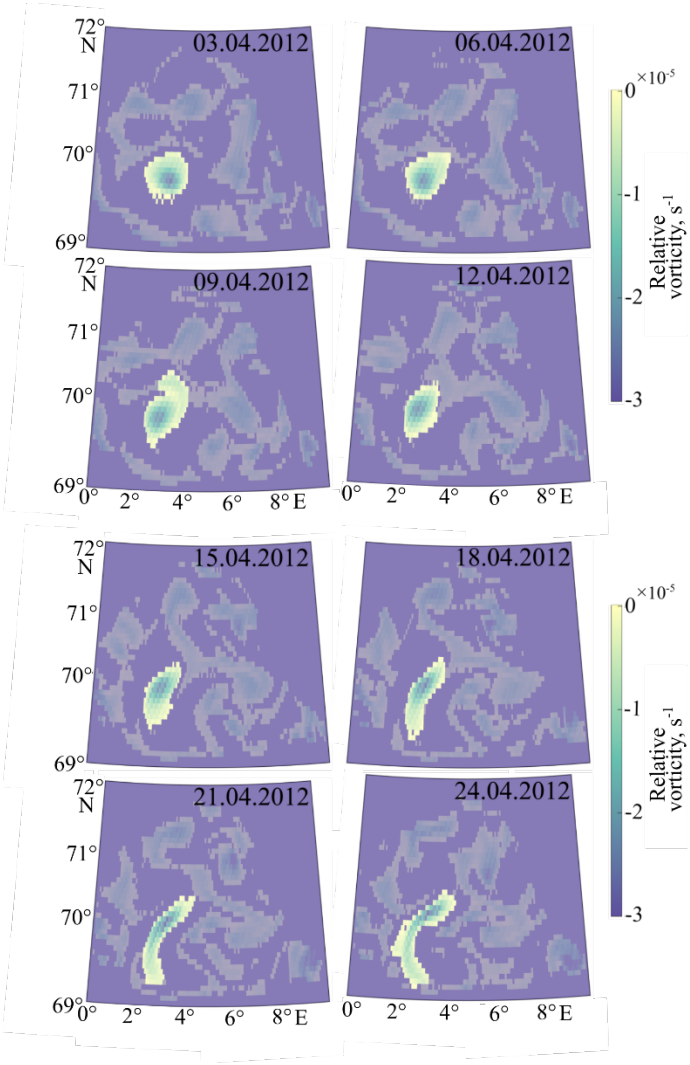

F i g. 1. Vortex evolution in the Lofoten basin on April 3–24, 2012. The scale shows the relative vorticity values, the horizon is 541 m

Fig. 2 shows the vortex characteristics: the elongation parameter and the effective radius $r_0 = \sqrt{ab}$. At the initial moment, the vortex is round, and ε = 1. During the life cycle, the vortex gradually elongates, so that its longitudinal scale becomes 4 times larger than the transverse one. Note, however, that in this case, the effective radius changes insignificantly, and its values at the beginning and the end of the vortex life cycle are similar.

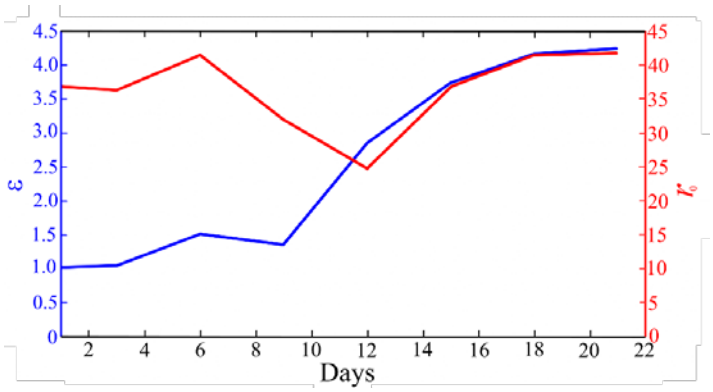

F i g. 2. Dimensionless parameter of the vortex horizontal elongation ε (blue curve) and its effective radius $r_0 = \sqrt{ab}$ (red curve). The *x*-axis shows the days of the vortex life cycle from the beginning of measurements on April 4–24, 2012

Fig. 3 shows the Väisälä-Brunt frequency and the dimensionless parameter of the vertical oblateness of the vortex core (in the calculations, the vertical semi-axis was assumed to be 400 m) [13]. It can be seen that both characteristics increase during the life cycle. The Väisälä-Brunt frequency increase is possibly associated with the observation period (April), i.e., the vortex life cycle takes place during the transition from winter to summer water stratification. At the beginning of the life cycle, winter stratification with the influence of winter convection is still preserved in the vortex, while towards the end of the cycle, water stratification intensifies [5] and the frequency *N* increases [16].

Let us show that an increase in the parameter *K* is associated with an increase in the Väisälä-Brunt frequency *N*. Let us express the size of the vertical semi-axis *c* in terms of the volume of the vortex core V_0 and the parameter $r_0 = \sqrt{ab}$. As a result, the following ratio is obtained

$$K = \frac{N}{f}\frac{3V_0}{4\pi r_0^3}. \qquad (7)$$

According to the estimates presented in Fig. 2, the characteristic effective radius r_0, although insignificantly, changes during the vortex deformation, but its initial and final values almost coincide. It is natural to assume that the vortex core volume V_0 also remains unchanged (or changes insignificantly). As a result, it turns out that the only parameter due to which *K* can change is the Väisälä-Brunt frequency *N*. The graph in Fig. 3 shows that the parameter *K* increases almost in phase with the Väisälä-Brunt frequency, which is also confirmed by formula (7). This gives reason to believe that the *K* increase is due solely to the *N* increase.

[5] Fedorov, A.M., Belonenko, T. and Bashmachnikov, I., 2019. Winter Convection in the Lofoten Basin According to ARGO Buoys and Hydrodynamic Modeling. *Vestnik of Saint Petersburg University. Earth Sciences*, 64(3), pp. 491-511. doi:10.21638/spbu07.2019.308 (in Russian).

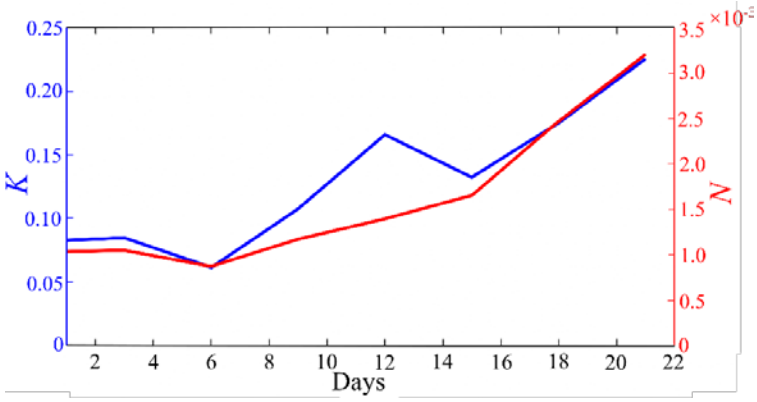

F i g. 3. Dimensionless parameter of the vortex core vertical oblateness *K* (blue curve) and the Väisälä-Brunt frequency *N* (red curve). The abscissa axis shows the days of the vortex life cycle from the beginning of measurements on April 4–24, 2012

Next, the estimates of the first (kinetic energy) and second (potential energy) terms in formula (1) are separately analyzed. In the horizontal plane, the integration region is limited by the vortex region (see Fig. 1); the depth integral is traditionally taken in the range of 0–1000 m (see review in [16]).

The results are given in Fig. 4. It can be seen that the potential energy of the vortex is 1.5 times higher than its kinetic energy. Let us note that during the vortex life cycle, its energy decreases, the kinetic energy decreases by 3 times, and the potential energy decreases by an average of 1.7 times. The total energy of the vortex decreased by 2.3 times. This energy decrease is associated with a change in the vortex shape and its elongation. The lower rate of decrease in potential energy compared to the kinetic energy is obviously related to the Väisälä-Brunt frequency. Its increase by the end of the period slows down the decrease in the potential energy of the vortex.

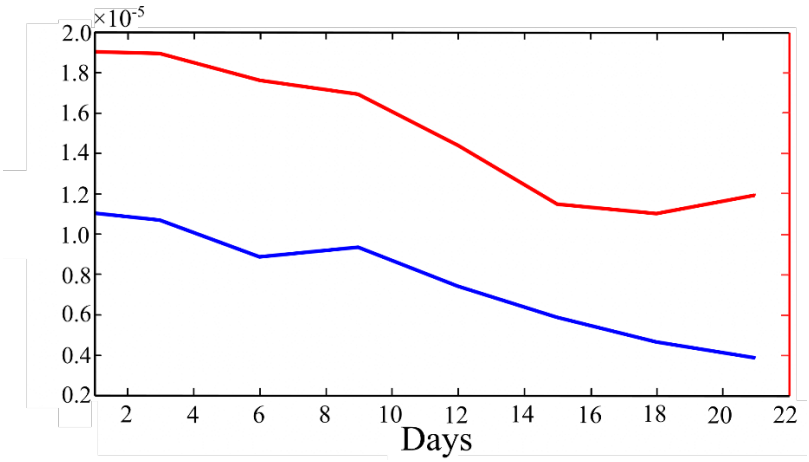

F i g. 4. Kinetic (blue curve) and potential (red curve) energy of the vortex (J). The *x*-axis shows the days of the vortex life cycle from the beginning of measurements on April 4–24, 2012

Fig. 5 shows the change in the potential and kinetic energy of the vortex depending on its horizontal elongation ε. Judging by the graphs, the energy decreases (almost linearly) with the elongation parameter increase.

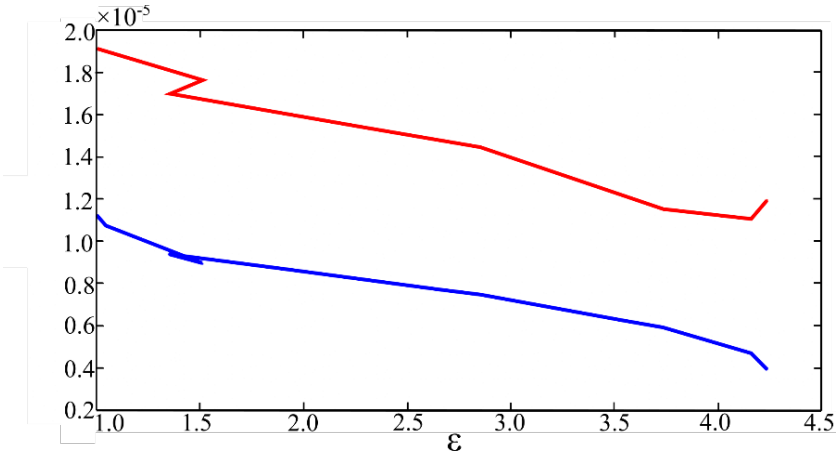

F i g. 5. Dependence of kinetic (blue curve) and potential (red curve) energy on the dimensionless parameter of horizontal elongation ε inferred from the *in-situ* data

According to Fig. 4 and 5, the total energy of the vortex decreased by about a factor of 2.3 when it was elongated. Let us now try, based on theoretical considerations, to estimate the reduction degree in the vortex energy $H(\varepsilon, K)$ due to changes in ε and K. During the considered life cycle, the vortex in the plane of parameters (ε, K) moved from the point (1; 0.08) to the point (4.3; 0.23). According to the *in-situ* data calculations (based on the *GLORYS12V1* reanalysis), the ratio of the final energy to its initial value is $\frac{H(4.3;0.23)}{H(1;0.08)} = \frac{1}{2.3} = 0.43$. Let us calculate the final energy of the vortex, normalized to its initial value, according to formulas (2), and (3), taking into account (4). As a result, we obtain $\frac{H(4.3;0.23)}{H(1;0.08)} = 0.80$. As can be seen, the calculated theoretical value $\frac{H(4.3;0.23)}{H(1;0.08)}$ differs from its practical estimate by almost a factor of two, with a qualitative agreement and a decrease in the energy of the vortex when it is elongated. Similarly, the decrease in the vortex core energy $H_{core}(\varepsilon, K)$ with a change in parameters (ε, K) according to formula (6) is calculated, taking into account (7), normalized to the initial value of the core energy: $\frac{H(4.3;0.23)}{H(1;0.08)} = 0.53$. It can be seen, when only the vortex core energy is taken into account, the relative energy loss of 0.53 became much closer to its practical value of 0.43. The difference can be explained by the fact that, apparently, when calculating the energy from *in-situ*

data, the core energy was mainly taken into account, while the energy of the external rotating fluid was ignored.

The calculation of the change in the relative kinetic energy of the core, according to the theoretical relation (4), gives the value of $\frac{H^k_{core}(4.3;0.23)}{H^k_{core}(1;0.08)} = 0.53$, its estimate from *in-situ* data is as 0.33. A similar theoretical change in the available potential energy, according to (5), is $\frac{H^p_{core}(4.3;0.23)}{H^p_{core}(1;0.08)} = 0.54$. A similar estimate based on *in-situ* data is 0.59. The estimates of the relative decrease coefficients in the vortex energy are given in the table.

Thus, a qualitative conclusion about the decrease in all types of energy of the vortex during its elongation can be made. This is true both theoretically and according to the *in-situ* data. Regarding quantitative estimates, we can speak of almost complete agreement between theoretical and practical calculations when the vortex core energy is estimated. The greatest difference between theoretical and practical estimates is observed in the change in the total energy of the vortex. Some quantitative differences in the estimates may be due to the inaccuracy of the practical determination of the vortex scales from *in-situ* data.

Coefficient estimates of relative attenuation of different types of vortex energy during its transition by the parameters (ε, K) from the state (1; 0.08) to the state (4.3; 0.23)

The relative total energy of the vortex $\frac{H(4.3;0.23)}{H(1;0.08)}$	The relative total energy of the vortex core $\frac{H_{core}(4.3;0.23)}{H_{core}(1;0.08)}$	The relative kinetic energy of the vortex core $\frac{H^k_{core}(4.3;0.23)}{H^k_{core}(1;0.08)}$	The relative available potential energy of the vortex core $\frac{H^p_{core}(4.3;0.23)}{H^p_{core}(1;0.08)}$
Based on *in-situ* data			
	0.43	0.33	0.59
Theory			
0.80	0.53	0.53	0.54

The vortex core transformation during its elongation is also confirmed by the analysis of changes in the thermohaline vortex characteristics during its evolution. From Fig. 6, showing the temperature profiles in the vortex (longitudinal sections), it can be seen that when the vortex is elongated, the core region limited by 5°C is compressed several times. And if at the initial moment of time (April 4, 2012), when the vortex still had a round shape, the 5°C isotherm extended up to

600 m, then by April 21 it extended up to ~ 300 m, i.e., the area bounded by this isotherm, was halved in depth. At the same time, the core region bounded by the 4.5°C isotherm, on the contrary, stretches along the vortex in the longitudinal direction when it is elongated. Similar changes characterize the location of isopycnas in sections (not shown). Let us note that in Fig. 6, the vortex is not an ellipsoid, but rather a semi-ellipsoid, however, there is no contradiction in this, since the theory of ellipsoidal vortices also extends to the cases of subsurface vortices, when a semi-ellipsoid is considered as a vortex model (see, e.g., [13]).

In this way, along with the kinetic and potential energy decrease in the vortex, the core, in which the region with maximum values decreases in size, but stretches with lower temperatures in the longitudinal direction of the vortex, is transformed.

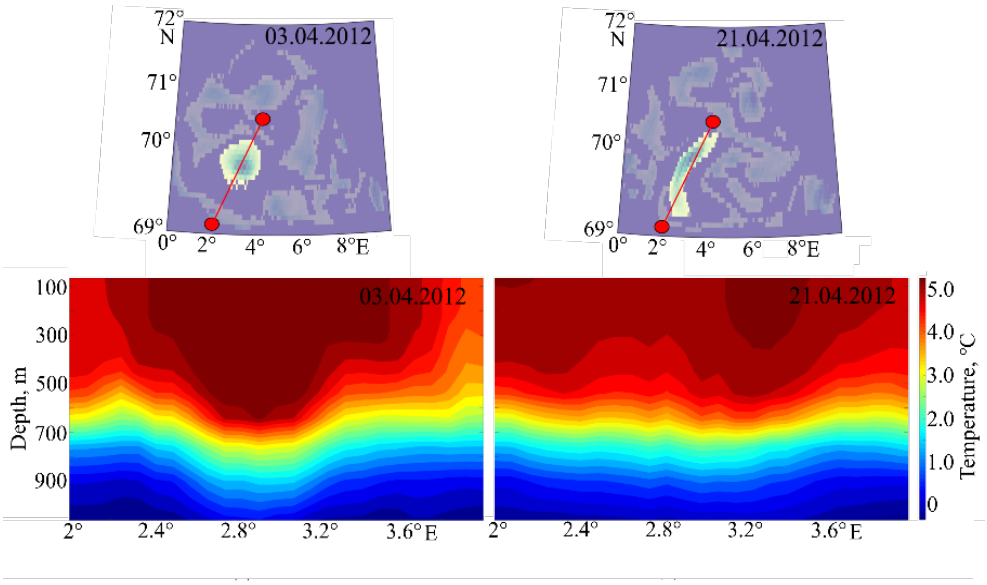

F i g. 6. Temperature profiles (vertical sections) (°C) in the vortex for April 3 and 21, 2012

Conclusions

The present work analyzes the transformation of the mesoscale vortex energy, which in the process of evolution changes its shape by elongation. From the analysis of the formulas, it follows that with such transformation, its kinetic and available potential energy decreases. It has also been established that when a vortex is deformed by a barotropic flow, the product of the horizontal semi-axes and, accordingly, the effective radius change insignificantly. The vortex energy change during its transformation is analyzed depending on the following parameters: ε, which characterizes the ratio of its horizontal axes, and $K = \frac{N}{f}\frac{c}{r_0}$ is the vortex oblateness parameter. The total mechanical energy of the vortex and separately its kinetic and available potential energy contained in the vortex core volume are

considered as functions of the parameters (ε, *K*). The energy decrease with increasing ε has been experimentally proven.

To verify the theoretical conclusions, the energy evolution of a mesoscale vortex located in the Lofoten basin of the Norwegian Sea is analyzed. The study was carried out according to the GLORYS12V1 reanalysis data. It is shown that in the course of evolution on April 4–24, 2012, the vortex, which initially had a round shape in the horizontal plane, is elongated, so that its longitudinal scale is 4 times greater than the transverse one. Let us note, however, that in this case, the effective radius changes insignificantly, and its values at the beginning and the end of the vortex life cycle are similar. It has been established that an increase in the *K* parameter of the considered vortex is associated with an increase in the Väisälä-Brunt frequency *N*.

A comparison of graphs of kinetic and potential energy shows that the potential energy of the vortex is 1.5 times higher than its kinetic energy. The energy decrease during the vortex transformation occurs in different ways: the kinetic energy decreases by 3 times, and the potential energy decreases by an average of 1.7 times. The total energy of the vortex decreased by 2.3 times. This energy decrease is associated with a change in the vortex shape and its elongation. An almost linear decrease in the potential and kinetic energy of the vortex is noted depending on the elongation parameter ε. Estimates of the coefficients of relative attenuation of various vortex energy types during its transition in terms of parameters (ε, *K*), made based on the *in-situ* data, qualitatively confirm the theoretical conclusions. The incomplete correspondence of quantitative estimates may be due to the inaccuracy of the practical determination of the current scales from *in-situ* data.

The theory of ellipsoidal vortices is currently the only theory that makes it possible to carry out an analytical study of vortices in the ocean. In this case, the analyzed characteristics, for example, energy, are described by cumbersome integrals. If the notion of mesoscale vortices as ellipsoidal is abandoned, we deal with integro-differential equations that are impossible not only to solve but even to make any estimates with their help. At the same time, we are confident that the use of the theory of ellipsoidal vortices has good prospects for the analysis, in particular, of mesoscale anticyclones in the ocean, and we have shown this in a number of papers. However, we are aware that such an analysis is limited by the quality of the data, on the one hand, and the concept of vortices as some kind of ideal geometric bodies, on the other.

REFERENCES

1. Kida, S., 1981. Motion of an Elliptic Vortex in a Uniform Shear Flow. *Journal of the Physical Society of Japan*, 50(10), pp. 3517-3520. https://doi.org/10.1143/JPSJ.50.3517
2. Zhmur, V.V., 2010. *Mesoscale Ocean Eddies*. Moscow: GEOS, 290 p. (in Russian).
3. Zhmur, V.V., Novoselova, E.V. and Belonenko, T.V., 2021. Potential Vorticity in the Ocean: Ertel and Rossby Approaches with Estimates for the Lofoten Vortex. *Izvestiya, Atmospheric and Oceanic Physics*, 57(6), pp. 632-641. doi:10.1134/S0001433821050157

4. Sandalyuk, N.V., Bosse, A. and Belonenko, T.V., 2020. The 3-D Structure of Mesoscale Eddies in the Lofoten Basin of the Norwegian Sea: A Composite Analysis from Altimetry and In Situ Data. *Journal of Geophysical Research: Oceans*, 125(10), e2020JC016331. https://doi.org/10.1029/2020JC016331

5. Ivanov, Iu.A., Kort, V.G., Monin, A.S., Ovchinnikov, I.M. and Shadrin, I.F., 1986. On the Mesoscale Inhomogeneities of the Ocean. *Doklady Akademii Nauk SSSR*, 289(3), pp. 706-709 (in Russian).

6. Kort, V.G., ed., 1988. [*Hydrophysical Studies under Mesopolygon Program*]. Moscow: Nauka, 263 p. (in Russian).

7. Kamenkovich, V.M., Koshlyakov, M.N. and Monin, A.S., eds., 1986. *Synoptic Eddies in the Ocean*. Dordrecht, Holland: Springer, 444 p. doi:10.1007/978-94-009-4502-9

8. Korotaev, G.K., 1957. [*Theoretical Modeling of Synoptic Variability of the Ocean*]. Kiev: Naukova Dumka, 160 p. (in Russian).

9. Korotaev, G.K. and Chepurin, G.A., 1984. [Model of Dynamics of an Isolated Baroclinic Vortex]. In: [*Ocean Dynamics Issues*]. Leningrad: Hydrometeoizdat, pp. 143-156 (in Russian).

10. McWilliams, J.C., 1985. Submesoscale, Coherent Vortices in the Ocean. *Reviews of Geophysics*, 23(2), pp. 165-182. doi:10.1029/RG023I002P00165

11. Polvani, L.M. and Flierl, G.R., 1986. Generalized Kirchhoff Vortices. *The Physics of Fluids*, 29(8), pp. 2376-2379. https://doi.org/10.1063/1.865530

12. Meacham, S.P., 1992. Quasigeostrophic, Ellipsoidal Vortices in a Stratified Fluid. *Dynamics of Atmospheres and Oceans*, 16(3-4), pp. 189-223. doi:10.1016/0377-0265(92)90007-G

13. Zhmur, V.V., Novoselova, E.V. and Belonenko, T.V., 2022. Peculiarities of Formation of the Density Field in Mesoscale Eddies of the Lofoten Basin: Part 2. *Oceanology*, 62(3), pp. 289-302. doi:10.1134/S0001437022030171

14. Gordeeva, S., Zinchenko, V., Koldunov, A., Raj, R.P. and Belonenko, T., 2021. Statistical Analysis of Long-Lived Mesoscale Eddies in the Lofoten Basin from Satellite Altimetry. *Advances in Space Research*, 68(2), pp. 364-377. doi:10.1016/j.asr.2020.05.043

15. Zinchenko, V.A., Gordeeva, S.M., Sobko, Yu.V. and Belonenko, T.V., 2019. Analysis of Mesoscale Eddies in the Lofoten Basin Based on Satellite Altimetry. *Fundamentalnaya i Prikladnaya Gidrofizika*, 12(3), pp. 46-54. doi:10.7868/S2073667319030067

16. Travkin, V.S. and Belonenko, T.V., 2021. Study of the Mechanisms of Vortex Variability in the Lofoten Basin Based on Energy Analysis. *Physical Oceanography*, 28(3), pp. 294-308. doi:10.22449/1573-160X-2021-3-294-308

About the authors:

Vladimir V. Zhmur, Head of the Laboratory, Chief Research Associate, P.P. Shirshov Institute of Oceanology, RAS (36 Nakhimovskiy Ave., Moscow, Russian Federation, 117997), Dr.Sci. (Phys.-Math), correspondent member of RAS, **ORCID ID: 0000-0001-8217-0932**, **WoS ResearcherID: P-9738-2015**, **Scopus Author ID: 6602162918**, zhmur-vladimir@mail.ru

Vladimir S. Travkin, Engineer-Researcher, Department of Oceanology, St. Petersburg State University (7–9 Universitetskaya Naberezhnaya, St. Petersburg, Russian Federation, 199034), v.travkin@spbu.ru

Tatyana V. Belonenko, Professor, Department of Oceanology, St. Petersburg State University (7–9 Universitetskaya Naberezhnaya, St. Petersburg, Russian Federation, 199034), Dr.Sci. (Geogr.), **ORCID ID: 0000-0003-4608-7781**, **WoS ResearcherID: K-2162-2013**, **Scopus Author ID: 6507005889**, t.v.belonenko@spbu.ru

David A. Arutyunyan, postgraduate student of Moscow Institute of Physics and Technology (9 Institutskiy Lane, Dolgoprudniy, Moscow Region, Russian Federation, 141701), arutyunyan.da@phystech.edu

Contribution of the co-authors:

Vladimir V. Zhmur – development of the method, participation in writing and editing the article

Vladimir S. Travkin – analysis of literature data, development of the method, analysis of the data, preparation of graphic material

Tatyana V. Belonenko – problem statement, formulation of purposes and objectives of the study, development of approaches to the analysis and the main text of the article

David A. Arutyunyan – derivation of energy conversion formulas

The authors have read and approved the final manuscript.
The authors declare that they have no conflict of interest.